Conformational behaviour of laterally dialkoxy branched mesogens. Part one

H. Allouchi[a]; A. Belaaraj[a]; M. Cotrait[a]; E. Lafontaine[b]; P. Judeinstein[c]; J. -P. Bayle[c]

[a] Universite Bordeaux I, [b] DGA/CTA, [c] Laboratoire de Chimie Structurale Organique,

PLEASE SCROLL DOWN FOR ARTICLE

Conformational behaviour of laterally dialkoxy branched mesogens. Part one

H. ALLOUCHI, A. BELAARAJ, M. COTRAIT

Laboratoire de Cristallographie et Physique Cristalline,
ERS CNRS 133. 351, Cours de la Libération, Université Bordeaux I,
33405 Talence Cedex, France

E. LAFONTAINE

DGA/CTA, 16 bis Avenue Prieur de la Côte d'Or, 94114 Arcueil Cedex, France

P. JUDEINSTEIN and J.-P. BAYLE*

Laboratoire de Chimie Structurale Organique, URA CNRS 1384,
Université Paris XI, Bât. 410. 91405 Orsay Cedex, France

The crystal structures of two mesogenic compounds having two neighbouring lateral alkoxy chains in the central part of the molecules have been solved. In both structures, the common four ring central core is extended and quite rigid with a total length close to 28.5 Å. All the molecules are strictly parallel because of the $P\bar{1}$ space group; the molecular arrangement is characteristic of a nematogenic system. In these structures, the lateral alkoxy chains are folded back to the core; they exhibit slightly different conformations and are quite disordered. The ^{13}C chemical shift of the first $-OCH_2-$ within the lateral chains can probe the mean conformation of the chain in the nematic phase. This chemical shift is independent of the compound. Nevertheless, in the solid phase, this chemical shift is dependent on small geometrical changes due to the influence of the oxygen in the neighbouring lateral chain. In addition, temperature cycling of the sample leads to different crystalline solid forms as evidenced by DSC and NMR studies.

1. Introduction

When the core anisotropy is rather large, a lateral flexible substituent can be introduced in a molecule without destroying the mesomorphic properties. It has been shown that this lateral chain adopts a special conformation in the liquid crystalline phase and is more or less oriented along the molecular long axis [1–10]. Recently, we have demonstrated that a second chain can be introduced near the first one if the core contains four rings [11]. In a ^{13}C NMR study, it was emphasized that the ordering behaviour of the two lateral alkoxy chains in the nematic phase is quite different from that seen in the case of terminal chains [12]. The first two carbons of the lateral alkoxy chains have a positive order parameter, indicating that the two chains are folded back along the mesogenic core. The order parameter values do not exhibit the well known odd–even effect with respect

to the chain carbon number and do not change significantly for each subsequent methylene carbon in each chain. Consequently, in the liquid crystalline phase, the conformational disordering does not increase along the chains as has been observed for terminal chains in conventional mesogens. This interesting behaviour is related to the lack of motional freedom of the chain folded back along a rigid core. The problem of the conformation of these chains in the solid phase is of interest, as the structure found in the crystalline phase is usually characteristic of the mesophase type. Therefore, in this work, the lateral chain conformations are investigated by X-ray for two single crystals having an odd and an even number of carbons in the lateral chains (namely 5DIAB and 6DIAB having, respectively, two pentyloxy and two hexyloxy chains). For compounds having a single chain, it was possible to correlate the structural information obtained by X-ray and by ^{13}C NMR in the solid phase. In fact, it was found that the ^{13}C signal of

*Author for correspondence; e-mail: jpbayle@icmo.u-psud.fr

the first carbon in the chain can be used to monitor the conformation of the first part of the chain. In, this paper, we will re-examine this possible correlation in these dilaterally substituted compounds.

2. Experimental

2.1. *Synthesis*

The compounds (5DIAB and 6DIAB) were prepared following an already published procedure [11, 12].

Two new compounds 4DIAE and 6DIAF were prepared similarly and were recrystallized from an acetonitrile/chloroform mixture (80/20) until constant transition temperatures were obtained. 6DIAF was synthesized to study the influence of the terminal parts of the mesogenic structure on the chain conformations and 4DIAE to consider the influence of short end chains on the conformations. The structures and the purity of the compounds were controlled using 1H NMR and a Bruker AM 250 spectrometer. The phase transitions were observed and characterized using an Olympus polarizing microscope fitted with an FP 82 Mettler heating stage and an FP 85 Mettler DSC without prior melting of the samples. These transition temperatures were recorded at a 10°C min^{-1} heating rate.

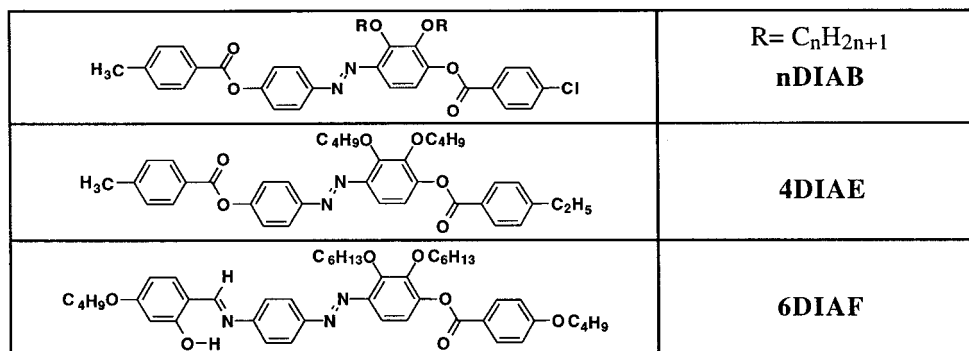### 2.2. *X-ray data collection and structure resolution*

Suitable crystals of 2,3-di-*n*-pentyloxy-4-(4-chlorobenzoyloxy)-4′-(4-methylbenzoyloxy)azobenzene (5DIAB) and 2,3-di-*n*-hexyloxy-4-(4-chlorobenzoyloxy)-4′-(4-methylbenzoyloxy)azobenzene (6DIAB) were grown at room temperature from CHCl$_3$ solution by slow evaporation. The crystal settings, the cell parameters and data collection were performed with a CAD-4 Enraf-Nonius diffractometer, equipped with a graphite monochromator.

The MoK$_\alpha$ and CuK$_\alpha$ radiations were used, respectively, for 5DIAB and 6DIAB. The crystal data, data collection and refinement characteristics are given in table 1. Respectively, 14 reflections with θ between 11° and 16° for 5DIAB and 23 reflections with θ between 25° and 41°

Table 1. Data collection and refinement characteristics for 5DIAB and 6DIAB.

Data collection	5DIAB	6DIAB
Chemical formula	C$_{37}$H$_{39}$ClN$_2$O$_6$	C$_{39}$H$_{43}$ClN$_2$O$_6$
Molecular weight (g mol^{-1})	643.2	671.2
Crystal system	triclinic	triclinic
Space group	P$\bar{1}$	P$\bar{1}$
Number of molecules per unit cell (Z)	2	2
a (Å)	16.753(2)	9.726(2)
b (Å)	11.774(2)	12.072(1)
c (Å)	9.297(7)	16.866(2)
α (°)	107.49(6)	94.22(1)
β (°)	86.28(7)	100.52(1)
γ (°)	101.47(6)	108.60(1)
Volume of cell (Å^3)	1714	1827
Density (g cm^{-3})	1.246	1.220
Radiation	MoK$_\alpha$	CuK$_\alpha$
Wavelength (Å)	0.7107	1.5418
Absorption μ (mm^{-1})	0.18	1.165
Crystal shape	prism	prism
Crystal colour	red	red
h_{min}, h_{max}	−17, 17	0, 12
k_{min}, k_{max}	−12, 12	−15, 15
l_{min}, l_{max}	−1, 9	−21, 21
θ_{max} (°)	22	65
Measured reflections	5162	7961
Independent reflections	4216	6570
Observed reflections	2754	5455
Criteria	$I > 3\sigma(I)$	$I > 3\sigma(I)$
R_{int} (%)	0.72	0.45
Refinement	on F^2	on F^2
Weight number of refined parameters	415	433
R	0.051	0.076
wR	0.056	0.083
S	2.59	2.53
Temperature (K)	293	293

for 6DIAB were used for the crystal settings and least-squares refinements of cell parameters. The absorption correction was performed using the Ψ scan technique [13].

Structure	
(structure with RO OR substituents, H$_3$C–benzoyloxy–azobenzene–benzoyloxy–Cl)	R= C$_n$H$_{2n+1}$ **nDIAB**
(structure with C$_4$H$_9$O OC$_4$H$_9$ substituents, H$_3$C–benzoyloxy–azobenzene–benzoyloxy–C$_2$H$_5$)	**4DIAE**
(structure with C$_6$H$_{13}$O OC$_6$H$_{13}$ substituents, C$_4$H$_9$O–benzylidene–azobenzene–benzoyloxy–OC$_4$H$_9$)	**6DIAF**

Both structures were solved by direct methods, using the Mithril package [14], which led to the positions of about two thirds of non-hydrogen atoms for both 5DIAB and 6DIAB. The remaining atoms were located after successive Fourier syntheses. A thorough examination of the density maps of 5DIAB showed that the end of one lateral pentyloxy chain, i.e. the propyl end, can occupy two different positions. Atomic parameters in both structures were refined with the SHELX93 package [15] with anisotropic thermal parameters for the non-hydrogen atoms, using constraints on the bond lengths of the hexyloxy chains in 6DIAB. The hydrogen atoms were required to ride on with the carbon atoms to which they are attached [15]. The final reliability factors were: $R = 0.051$ and 0.076; $wR = 0.056$ and 0.083 with a goodness of fit: $S = 2.59$ and 2.53, respectively for the 5DIAB and 6DIAB structures. The rather high values of the R and wR factors for the 6DIAB structure can be related to some disorder and high thermal motion factors. The atomic scattering factors were taken from the International Tables for X-ray Crystallography (1974, Vol. IV).

2.3. *^{13}C NMR spectra in the solid and nematic phase*

High resolution ^{13}C NMR results were obtained with a Bruker MSL 200 spectrometer with quadrature detection using a double-tuned coil for ^{13}C and ^{1}H NMR. The crystalline samples were filled into fused zirconia rotors fitted with boron nitride caps and spun at 6 kHz at the magic angle (54.7°). ^{13}C chemical shifts were referenced to the glycine carbonyl signal (assigned at 176.03 ppm) used as an external reference. The spectra were obtained using a cross-polarization pulse (with a ^{1}H 90° pulse of 4.1 µs), high power decoupling during acquisition, 0.03 s acquisition, 3 s recycle delay, 512 scans and 1.2 ms mixing time. Variable temperature CP/MAS NMR experiments were performed in the 30–150°C range using a Eurotherm thermal controller, calibrated with the DABCO (1,4-diazabicyclo-(2,2,2)-octane) crystal–crystal transition [16].

3.   Results and discussion
3.1. *Transition temperatures*

The transition temperatures of the *n*DIAB homologues ($n = 4, 5, 6$), 4DIAE and 6DIAF are given in table 2.

For 4DIAE, the transition temperatures are close to those of 4DIAB. The replacement of the terminal chlorine atom by the ethyl group does not influence the thermodynamic stability of the mesophase. This interesting feature was also observed when the polar atom was introduced on a lateral aromatic branch [10].

6DIAF has a central core part identical to 6DIAB. Nevertheless, the rigidity of the left far part of the

Table 2.   Transition temperatures (°C) for the different compounds synthesized.

n	Cr	→	N	→	I
4DIAB	•	117	•	183.5	•
5DIAB	•	99.5	•	160	•
6DIAB	•	86.5	•	140.5	•
4DIAE	•	122	•	185	•
6DIAF	•	62	•	198	•

molecule is increased due to intramolecular hydrogen bonding between the hydrogen of the hydroxyl group and the nitrogen atom of the imine bond. As a consequence, the nematic range of 6DIAF is larger than that of 6DIAB. This effect has to be related to the more rigid link which certainly, in the nematic phase, decreases the conformational disordering of the lateral chains. In some laterally substituted compounds having the same number of lateral chains, but differing in the link type, it has been clearly observed that the nematic range is enhanced through the rigidity of the links [17]. The two short butoxy terminal chains may also help by increasing the longitudinal molecular anisotropy.

3.2. *Structure analysis*

The fractional atomic coordinates and the equivalent Beq factors are given in table 3 for 5DIAB and table 4 for 6DIAB. The Beq factors of the polyaromatic cores in both compounds are rather low. Those of the lateral alkoxy chains are slightly higher for 5DIAB and much higher for 6DIAB. For the latter compound, the Beq factors increase to a large extent from the beginning to the end of the hexyloxy chains, to the extent that such chains can be considered quite disordered. In 5DIAB there are two statistical positions for one of the lateral pentyloxy chains, defined by the atoms C46, C47, C48 on one side and C146, C147, C148 on the other side. The labelling of non-hydrogen atoms and the SNOOPI [18] drawings of both conformations of a 5DIAB molecule are presented in figures 1(*a*) and 1(*b*). In figure 1(*c*) the SNOOPI drawing of a 6DIAB molecule is displayed. In the 6DIAB molecule, the thermal ellipsoids for the terminal atoms of the lateral chains are quite large, indicating that the hexyloxy chains are rather disordered.

All benzene rings are perfectly planar as well as the C20−N=N−C13 group, but the ϕ−N=N−ϕ fragment is not at all planar. The aromatic rings are designated as ϕ1 (atoms C1 to C6), ϕ2 (atoms C10 to C15), ϕ3 (atoms C20 to C25) and ϕ4 (atoms C30 to C35). The benzoate groups are quite planar. The dihedral angles between contiguous phenyl ring mean-planes are given in table 5. Taking into account the bulkiness of the terminal Cl and CH$_3$ groups, the length of the polyaromatic core is close to 28.5 Å. This length is independent of the

Table 3. Fractional atomic coordinates and Beq factors for 5DIAB.

Atom	x/a	y/b	z/c	Beq/Å²
C1	−0.4816(4)	−1.2241(6)	−0.0896(10)	8.5(4)
C2	−0.5025(4)	−1.1512(7)	0.0471(10)	8.4(4)
C3	−0.4490(4)	−1.0485(6)	0.1240(8)	6.3(3)
C4	−0.3737(3)	−1.0168(5)	0.0610(7)	5.0(3)
C5	−0.3518(4)	−1.0895(5)	−0.0781(8)	6.3(3)
C6	−0.4068(5)	−1.1940(6)	−0.1535(10)	8.5(4)
C7	−0.3194(3)	−0.9040(5)	0.1490(7)	4.7(2)
O8	−0.2522(2)	−0.8792(3)	0.0651(4)	5.9(2)
O9	−0.3318(2)	−0.8425(4)	0.2711(5)	6.4(2)
C10	−0.1926(3)	−0.7760(5)	0.1305(6)	4.9(2)
C15	−0.1438(4)	−0.7774(5)	0.2422(7)	5.1(3)
C14	−0.0802(3)	−0.6801(5)	0.2920(6)	4.7(2)
C13	−0.0680(3)	−0.5854(4)	0.2284(6)	4.0(2)
C12	−0.1190(3)	−0.5868(5)	0.1154(6)	4.6(2)
C11	−0.1815(3)	−0.6833(5)	0.0661(7)	4.9(3)
N16	0.0016(3)	−0.4914(4)	0.2847(5)	4.4(2)
N17	0.0066(3)	−0.4001(4)	0.2414(5)	4.1(2)
C18	−0.5423(6)	−1.3360(7)	−0.1730(15)	13.7(6)
C20	0.0787(3)	−0.3118(5)	0.2933(6)	3.9(2)
C21	0.1483(3)	−0.3402(5)	0.3378(6)	4.5(2)
C22	0.2170(3)	−0.2524(5)	0.3782(7)	4.8(3)
C23	0.2147(3)	−0.1369(5)	0.3752(6)	4.3(2)
C24	0.1475(3)	−0.1043(5)	0.3319(6)	3.9(2)
C25	0.0784(3)	−0.1943(5)	0.2879(6)	3.6(2)
C27	0.2856(3)	0.0325(5)	0.5543(7)	4.5(2)
O26	0.2869(2)	−0.0482(3)	0.4146(4)	5.1(2)
O28	0.2304(2)	0.0296(3)	0.6400(4)	5.4(2)
Cl29	0.5919(1)	0.3991(2)	0.7149(3)	10.4(1)
C30	0.3636(3)	0.1246(5)	0.5851(7)	4.3(2)
C31	0.3657(3)	0.2219(5)	0.7128(7)	5.5(3)
C32	0.4353(4)	0.3075(5)	0.7507(8)	6.1(3)
C33	0.5029(4)	0.2932(5)	0.6599(8)	6.3(3)
C34	0.5033(4)	0.1975(6)	0.5309(9)	7.7(3)
C35	0.4310(4)	0.1115(6)	0.4935(7)	6.1(3)
O36	0.1521(2)	0.0117(3)	0.3291(4)	4.5(2)
C37	0.0959(3)	0.0769(5)	0.4309(7)	5.3(3)
C38	0.1146(4)	0.2067(5)	0.4283(7)	5.8(3)
C39	0.1960(4)	0.2755(6)	0.4921(8)	6.5(3)
C40	0.2131(5)	0.4081(6)	0.4995(9)	7.9(4)
C41	0.2877(6)	0.4786(7)	0.5789(10)	10.4(5)
O43	0.0092(2)	−0.1687(3)	0.2462(4)	4.0(1)
C44	0.0139(4)	−0.1506(5)	0.0992(7)	5.1(3)
C45	−0.0668(4)	−0.1342(6)	0.0626(7)	6.0(3)
C46	−0.1215(7)	−0.2732(11)	0.0268(15)	6.1(6)
C47	−0.2088(7)	−0.2569(13)	−0.0196(16)	6.1(6)
C48	−0.2628(8)	−0.3829(12)	−0.0502(15)	6.6(6)
C146	−0.1449(8)	−0.2161(12)	0.0691(16)	6.9(6)
C147	−0.1542(11)	−0.3265(14)	−0.0432(16)	9.3(8)
C148	−0.2434(8)	−0.4147(13)	−0.0318(19)	8.1(8)

Table 4. Fractional atomic coordinates and Beq factors for 6DIAB.

Atom	x/a	y/b	z/c	Beq/Å²
C1	−0.8289(11)	−1.2061(7)	−0.9505(6)	7.7(4)
C2	−0.6904(11)	−1.1570(8)	−0.9678(5)	7.8(4)
C3	−0.5821(10)	−1.0624(7)	−0.9167(5)	6.8(4)
C4	−0.6102(10)	−1.0132(6)	−0.8470(5)	5.9(3)
C5	−0.7497(10)	−1.0639(7)	−0.8282(5)	6.5(3)
C6	−0.8549(10)	−1.1589(7)	−0.8790(6)	7.2(4)
C7	−0.4945(10)	−0.9091(6)	−0.7985(5)	6.0(3)
O8	−0.5443(5)	−0.8690(4)	−0.7337(3)	5.0(2)
O9	−0.3740(7)	−0.8610(5)	−0.8109(4)	8.4(3)
C10	−0.4497(10)	−0.7666(6)	−0.6803(5)	6.3(3)
C15	−0.3187(10)	−0.7623(7)	−0.6340(5)	6.7(3)
C14	−0.2410(10)	−0.6639(7)	−0.5756(5)	6.6(3)
C13	−0.2976(9)	−0.5747(6)	−0.5654(5)	5.7(3)
C12	−0.4321(10)	−0.5804(6)	−0.6137(5)	6.3(3)
C11	−0.5100(10)	−0.6775(7)	−0.6713(5)	6.7(3)
N16	−0.2110(8)	−0.4818(5)	−0.5008(4)	6.4(3)
N17	−0.2556(7)	−0.3949(5)	−0.4965(4)	5.9(2)
C18	−0.9482(13)	−1.3073(9)	−1.0069(7)	9.9(5)
C20	−0.1734(9)	−0.3081(6)	−0.4272(5)	5.9(3)
C21	−0.0940(11)	−0.3350(7)	−0.3589(5)	7.0(4)
C22	−0.0265(11)	−0.2526(8)	−0.2910(5)	7.8(4)
C23	−0.0320(10)	−0.1383(7)	−0.2948(5)	7.1(4)
C24	−0.1083(9)	−0.1085(6)	−0.3617(5)	5.8(3)
C25	−0.1821(9)	−0.1945(6)	−0.4299(5)	5.6(3)
O26	0.0293(8)	−0.0596(6)	−0.2231(4)	9.3(3)
C27	0.1568(13)	0.0197(9)	−0.2189(6)	8.7(5)
O28	0.2203(9)	0.0304(7)	−0.2752(5)	10.7(4)
Cl29	0.4137(6)	0.3417(4)	0.0965(3)	17.8(3)
C30	0.2172(12)	0.0983(9)	−0.1368(6)	8.4(4)
C35	0.1666(12)	0.0611(9)	−0.0716(8)	9.8(5)
C34	0.2259(14)	0.1325(11)	0.0077(7)	10.3(6)
C33	0.3327(12)	0.2449(9)	0.0092(6)	9.0(5)
C32	0.3730(13)	0.2737(9)	−0.0611(7)	9.9(5)
C31	0.3192(15)	0.2002(9)	−0.1327(6)	10.1(5)
O36	−0.1159(6)	0.0042(4)	−0.3589(3)	6.4(2)
C37	−0.0434(11)	0.0750(7)	−0.4138(5)	7.3(4)
C38	−0.0416(12)	0.1987(8)	−0.3957(5)	7.5(4)
C39	0.0653(13)	0.2626(8)	−0.3161(6)	8.4(4)
C40	0.0736(13)	0.3859(8)	−0.2949(7)	9.5(5)
C41	0.1816(15)	0.4423(10)	−0.2129(8)	12.1(6)
C42	0.1803(16)	0.5619(11)	−0.1926(10)	13.9(8)
O43	−0.2538(6)	−0.1690(4)	−0.4990(3)	5.8(2)
C44	−0.3930(11)	−0.1535(8)	−0.4966(6)	7.5(4)
C45	−0.4613(13)	−0.1381(11)	−0.5796(7)	9.9(6)
C46	−0.5041(18)	−0.2510(17)	−0.6378(8)	16.6(10)
C47	−0.6049(15)	−0.2860(12)	−0.7135(10)	13.9(8)
C48	−0.6376(16)	−0.4096(12)	−0.7602(9)	12.8(7)
C49	−0.7356(20)	−0.4212(15)	−0.8417(13)	18.0(11)

compound, because the molecules are extended in the same way and the chains which overlap the core are not long enough to come out of the core. This can explain why every additional carbon in the lateral chains has only a slight additional perturbative effect on the liquid crystal properties compared with the opposite trends when carbons are added to terminal chains.

Interesting torsional angles for both 5DIAB conformers and for the 6DIAB molecule are presented in table 6.

The O−C−C−C torsional angles are equal to −66.2° and 71° for alkoxy chain C (see figure 1, atoms O36 to C41 or C42) for the 5DIAB and 6DIAB molecules, respectively. Now, because there are two conformers for
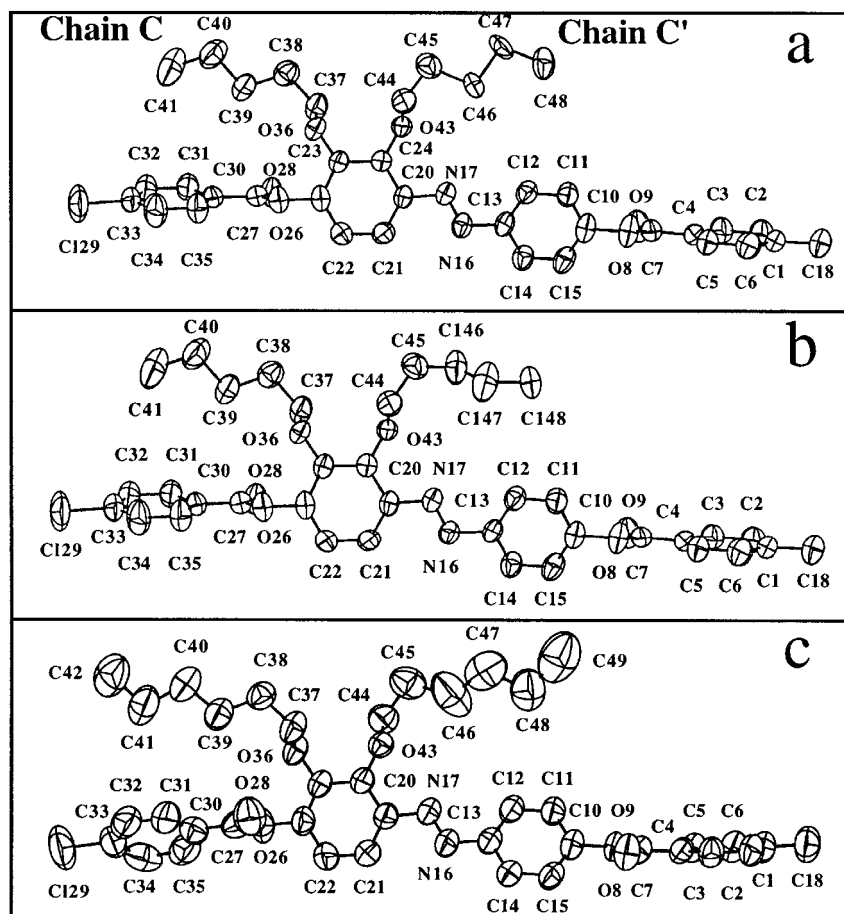
Figure 1. (*a, b*) SNOOPI drawings of the 5DIAB molecule. Displacement ellipsoids are drawn at the 50% probability level, (*a*) with C46, C47, C48 atoms (first conformation), (*b*) with C146, C147, C148 atoms (second conformation). (*c*) SNOOPI drawing of the 6DIAB molecule.

Table 5. Dihedral angles between contiguous rings mean-planes in 5DIAB and 6DIAB.

Compound	5DIAB	6DIAB
$\phi2/\phi1$	76.0°	59.8°
$\phi3/\phi2$	31.4°	31.0°
$\phi4/\phi3$	82.5°	57.8°

chain C′ (atoms O43 to C48 or C148) in the 5DIAB structure, the O–C–C–C angle is thus equal to −73.2° and −52.0° for the two 5DIAB conformers and 67° for the 6DIAB molecule.

In the 5DIAB molecule, the pentyl terminal part of the alkoxy lateral chain C and the first conformer of chain C′ are fully extended, but that is not the case for chain C′ in the second conformer. Thus, the chain lengths (taking into account the bulky terminal CH$_3$ group) are close to 7.25 and 7.35 Å; that of the second conformer of the pentyl chain is close to 6.8 Å. The hexyl parts of the hexyloxy lateral chains in 6DIAB are both close to 8.8 Å. The lateral alkoxy chains C and C′ in both molecules are folded back to the core and tightly packed with it, as is assumed to be true in the nematic

phase of this kind of compound [12]. The first pentyloxy chain C (atoms O36 to C41) and the first conformer of the pentyloxy chain C′ (atoms O43 to C48) present a *tgtt* conformation. Due to these peculiar conformations, C37 and C44 point in opposite directions above and below the mean plane of ring 3. The whole molecules of both 5DIAB and 6DIAB have no bulky group protruding from the core. This is in agreement with the existence of a nematic phase and may also explain the mesomorphic behaviour of compounds with one long lateral alkoxy chain [1–10].

The projection of the 5DIAB crystal structure (for the sake of clarity, only the first conformer is represented) on the (*x*O*y*) plane is shown in figure 2 (*a*). The polyaromatic cores are strictly parallel because of the space group. There are dipolar interactions between neighbouring COO polar groups of antiparallel molecules and numerous weak van der Waals interactions.

The projection of the 6DIAB crystal structure on the (*y*O*z*) plan is shown in figure 2 (*b*). It is quite similar to that of the 5DIAB structure. This molecular arrangement is characteristic of the nematic mesophase. At the melting temperature, molecules are expected to move freely with respect to each other, but we can expect that the lateral
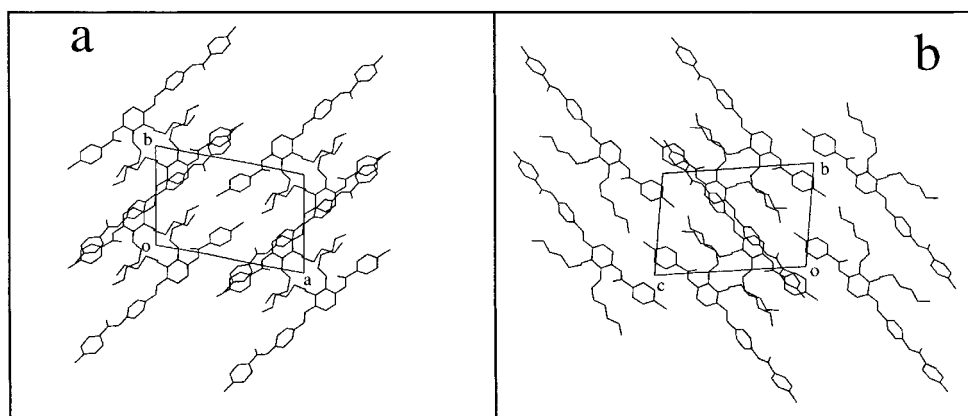
Figure 2. (*a*) Projection of the 5DIAB structure along the *c* axis. (*b*) Projection of the 6DIAB structure along the *a* axis.

Table 6. Interesting torsional angles for 5DIAB and 6DIAB molecules.[a]

Torsion angle		5DIAB	6DIAB
C3–C4–C7–O8		*trans*	*trans*
C7–O8–C10–C11		− 114.1(6)	124.6 (8)
C14–C13–N16–N17		*trans*	*trans*
N16–N17–C20–C25		− 162.2(5)	161.0(8)
C22–C23–O26–C27		− 104.7(6)	104.9(9)
C26–C27–C30–C31		*trans*	− 160(1)
C23–C24–O36–C37		− 118.2(6)	115(1)
C24–O36–C37–C38		*trans*	*trans*
O36–C37–C38–C39		− 66.2(6)	71(1)
C37–C38–C39–C40		*trans*	*trans*
C38–C39–C40–C41		*trans*	*trans*
C39–C40–C41–C42		—	*trans*
C20–C25–O43–C44		− 108.6(5)	109(1)
C25–O43–C44–C45		*trans*	*trans*
O43–C44–C45–C46	(1)[b]	− 73.2(7)	67(1)
C44–C45–C46–C47	(1)	*trans*	161(1)
C45–C46–C47–C48	(1)	*trans*	*trans*
C46–C47–C48–C49		—	*trans*
O43–C44–C45–C146	(2)[c]	− 52(1)	—
C44–C45–C146–C147	(2)	− 71(1)	—
C45–C146–C147–C148	(2)	*trans*	—

[a] Angles that differ by less than 10° from the *trans*-conformation (180°) are labelled '*trans*'.
[b] (1) denotes conformer 1 of 5DIAB.
[c] (2) denotes conformer 2 of 5DIAB.

chains will stay folded back along the core. This folding will keep the proper packing needed for the existence of the mesophase. In addition, this folding explains why the disordering increase along the lateral chain is weak.

The crystal packing in both structures is quite loose, corresponding to the rather low density (see table 1). This is a general feature in mesogenic structures with quite long alkyl or alkoxy chains [19, 20].

3.3. ^{13}C NMR spectra for the solid and nematic phases of the previously unmelted compounds

Recently, we have shown on compounds having a single lateral chain that it is possible to probe the lateral chain conformation by ^{13}C NMR using the −OCH$_2$− resonance in the solid and nematic phases [21, 22]. In these series, a downfield jump is observed when the lateral chain conformation changes in order to align the chain along the core in the liquid crystalline phase. These chemical shift differences were interpreted on the basis of the γ-*gauche* effect. In the compounds 5DIAB and 6DIAB, we expected a similar behaviour of the −OCH$_2$− peaks in the solid and nematic phases in accordance to the fact that the first fragments of the chains are already in *gauche*-conformation in the solid phase. It was thus surprising to obtain the two different NMR spectra presented in figures 3(*a*) and 7(*a*). In the −OCH$_2$− region, a single peak is observed in 5DIAB and two peaks are seen in 6DIAB indicating that if the two chains have nearly identical conformation, the folding of the chain is not the only factor to influence the chemical shift of the first carbon within the chains in the solid phase.

Let us consider the two MAS NMR spectra of 6DIAB (figure 3), below and above the solid–nematic transition, which were obtained without any prior melting of the sample. In the solid phase, the peaks are quite narrow with the exception of the protonated carbons of the *para*-disubstituted rings which indicates their rotation around the *para*-axes at a rate near the spinning frequency. No extra peaks are present in the spectrum, indicating that all the molecules have the same local environment. A single peak is observed in the −OCH$_2$− region and all the chain peaks are resolved in the solid phase (with the exception of C1, C1′ and C6, C6′ peaks).
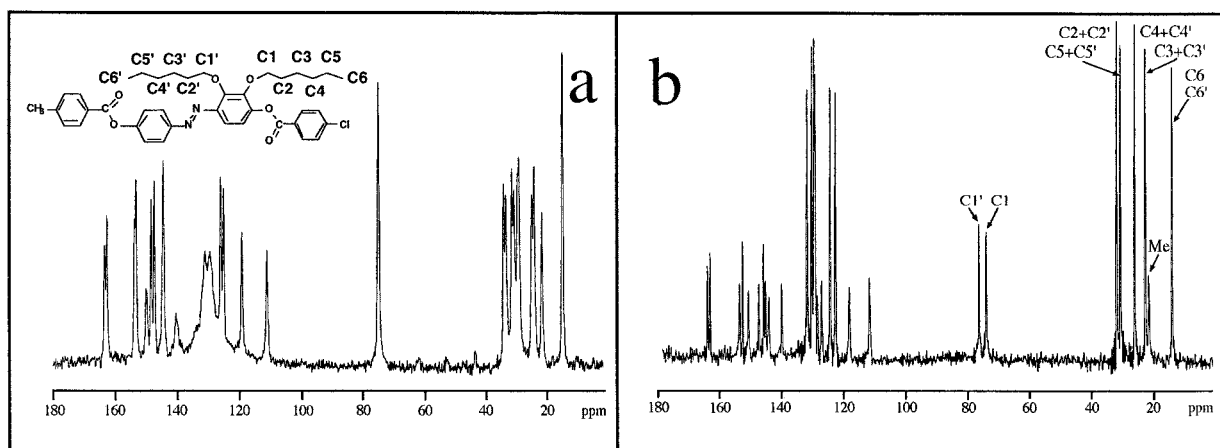
Figure 3. 50 MHz hydrogen decoupled ^{13}C MAS NMR of 6DIAB (*a*) in the solid phase 5°C below the solid–nematic transition; (*b*) in the nematic phase 5°C above the solid-nematic transition. The assignment is based on our previous study in the liquid crystalline phase [12].

In the nematic phase, chain carbons having identical position within the chains have the same chemical shifts and conversely two peaks are obtained for the $-OCH_2-$ carbons.

Figure 4 gives a better view of what is happening in the chemical shifts evolution with temperature for C1′ and C1 carbons in the 5DIAB and 6DIAB samples. Below the solid–nematic transition, a continuous down-field change is shown for resonances of both compounds on increasing the temperature. In the solid phase, the chain is locked in a particular conformation, giving a particular chemical shift value which can be influenced by the packing arrangement of the chains. We can conclude that no change in the chain conformation and packing occurs in the solid phase. But, in the solid phase, the $-OCH_2-$ resonance frequencies of both compounds are quite different, showing that the $-OCH_2-$ electronic environments differ in the two compounds.

The compounds were recrystallized again in another solvent mixture (ethanol/chloroform) and identical DSC curves and NMR results were obtained. As the conformations of the chains are quite equivalent in the two structures, the difference in the chemical shift can be attributed to the change of electronic density coming from nearby atoms. Certainly, the major influence derives from one lone pair of the oxygen of the nearby chain. Due to the particular conformations of the two chains, one lone pair is pointing in the direction of the first CH_2 belonging to the other chain. A small geometrical change within the two compounds (for instance the C23−C24−O36−O37 torsional angle) can lead to a modification in the interaction between the two fragments and then a difference in the chemical shift. Therefore, as the two chains interact, the chemical shift of the first carbon cannot be used to monitor the folded conformation of the chain.
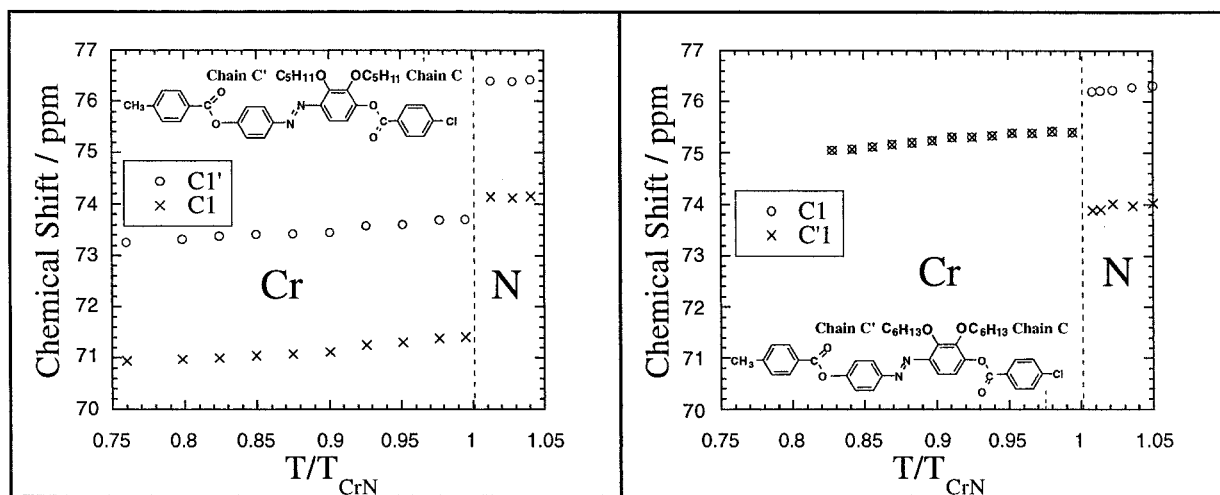

Figure 4. Chemical shift dependence of the lateral $-OCH_2-$ carbons in 5DIAB and 6DIAB on increasing the temperature.
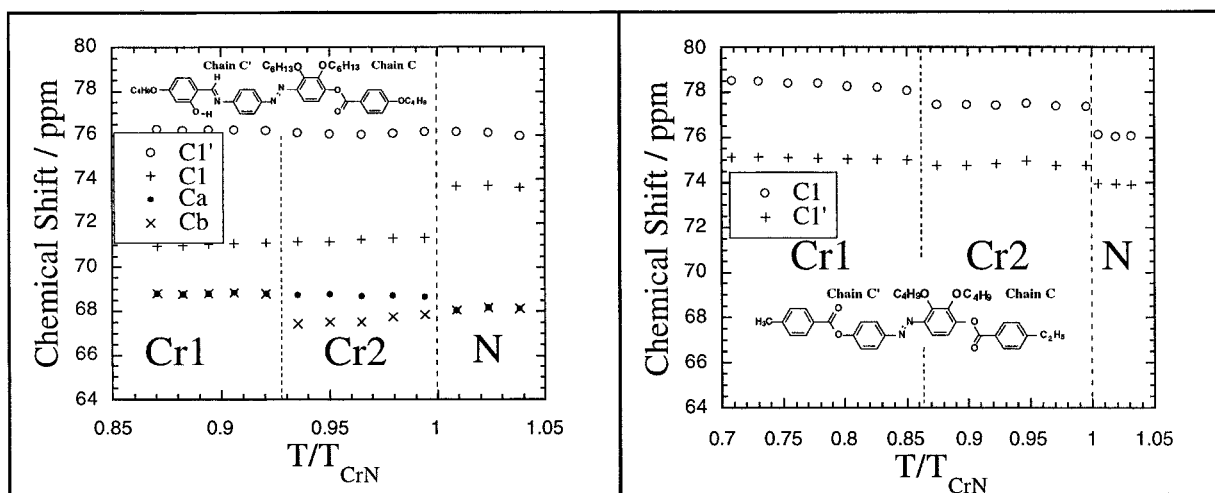
Figure 5.   Chemical shift dependence of the lateral $-OCH_2-$ carbons in (*a*) 6DIAF and (*b*) 4DIAE on increasing temperature. Assignment of Ca and Cb in 6DIAF may be inverted.

After the solid–nematic transition, the chemical shift pattern (figure 4) is the same for both compounds, indicating that in the nematic phase the mean conformation of the first fragment is independent of the chain length. The constant chemical shift of the first carbon in the lateral chain has already been noticed for other lateral alkoxy substituted compounds [21–23]. In addition, the isotropic chemical shifts (in $CDCl_3$ solution) are the same for the two compounds (74.40 and 76.04 ppm) and are assigned to the C1′ and C1 carbons, respectively [12]. In the nematic phase or in solution, the chemical shift is an average over all the populated conformations. As chemical shifts of the methyleneoxy carbons have similar values in solution or in the nematic phase, their mean conformations should be nearly identical. In fact, as these carbons are greatly hindered, the number of populated conformations is definitively low.

Figure 5 presents the chemical shift dependence of the lateral $-OCH_2-$ carbons in 6DIAF and 4DIAE with increasing temperature. As can be seen, the chemical shift dependence is different from those observed for 5DIAB and 6DIAB (figure 4), indicating again the difference of the electronic environment for the first fragment of the lateral chain in the solid phase. Nevertheless, the chemical shift of these carbons in the liquid crystalline phase is independent of the compound and identical to that observed for the 5DIAB and the 6DIAB molecules: i.e. 74.0 ± 0.1 and 76.2 ± 0.1 ppm for C1 and C1′ carbons, respectively. Thus, the mean conformation of the first carbons in the lateral chains is not influenced by the chain length and the far part of the core.

3.4. *Thermal behaviour upon temperature cycling*

On cooling, the NMR spectra of the samples are more complex, indicating that several different types of solid

can be obtained. In order to probe the difference between these solids, we have studied the thermal behaviour of the compounds upon temperature cycling. We will present the results for the compound 5DIAB (figure 6). Similar behaviours are obtained for the other compounds. Upon temperature cycling, significant differences are observed in the thermograms on increasing temperature before and after the sample has been melted and crystallized.

During the first heating at $15°C\,min^{-1}$ on the previously unmelted compound (called Cr1), the solid–nematic transition appears at 99.5°C, table 1, figure 6(*a*). After cooling and keeping the compound at 30°C or 40°C for different periods of time, the thermograms were also recorded at $15°C\,min^{-1}$ and are presented with the
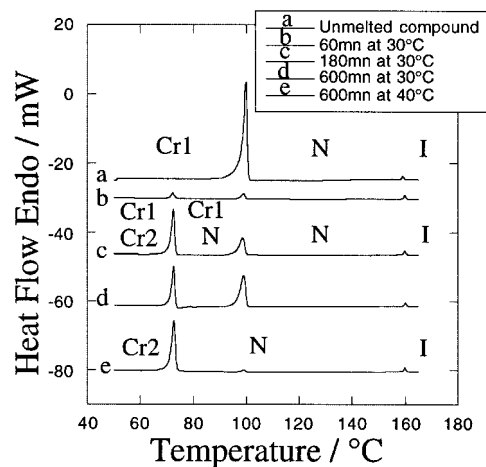

Figure 6.   Successive thermograms of 5DIAB. (*a*) Unmelted powder sample (or single crystals), (*b*–*e*) the sample was subjected to melting and was then cooled to 30°C or 40°C and held there for different times before the thermograms were recorded.
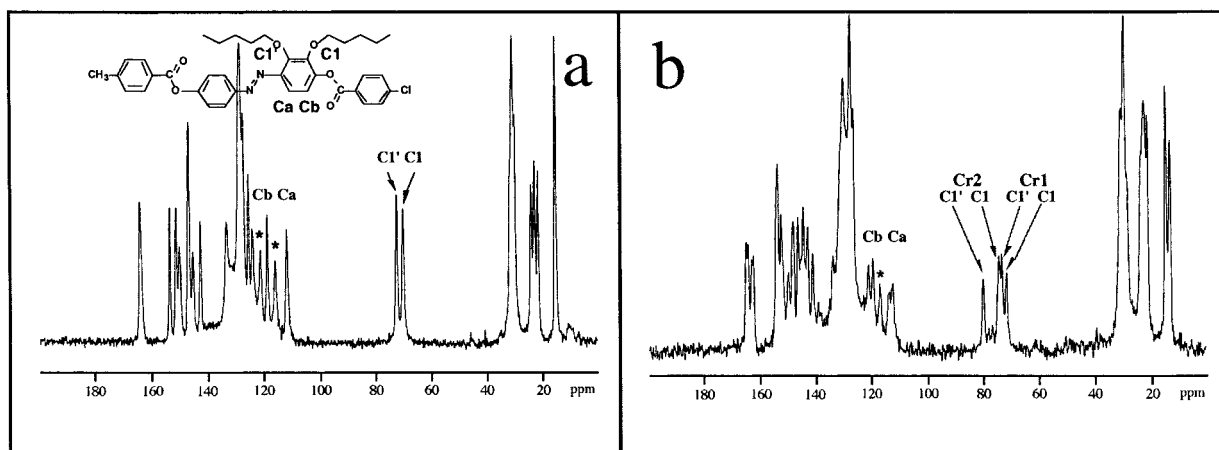
Figure 7.   50 MHz hydrogen decoupled ^{13}C MAS NMR of 5DIAB (*a*) in the solid phase at room temperature for the unmelted compound, (*b*) in the solid phase at room temperature after cycling the sample inside the rotor. *Indicates peaks related to the *para*-disubstituted aromatic rings; they disappear on heating.

same absolute scale. On thermogram (*b*) two very small peaks are obtained below 100°C showing that the compound is still mainly in a supercooled mesophase. The high temperature peak corresponds to that observed on thermogram (*a*). A new peak appears at 74.5°C, showing a decrease of nearly 25°C in comparison with the temperature obtained in the first run. This new peak indicates that a new solid (Cr2) is formed during the crystallization process. By allowing time for the crystallization process to occur, these two peaks gain in intensity. If the sample is kept at 40°C for 600 min, the second solid (Cr2) can be obtained quantitatively (*e*). We note that the clearing temperature on each thermogram remains the same at 160°C, indicating that no chemical change is involved in the modification of the thermogram. This shows clearly that at least two kinds of structurally different solids (Cr1 and Cr2) can be obtained, depending on the thermal history of the compound. This type of solid polymorphism has already been observed for other dilaterally substituted compounds [24].

Can we check the existence of these two solids by NMR? A sample of 5DIAB was melted inside the rotor, cooled rapidly and left inside an oven for two days at 40°C. Then the rotor was introduced at room temperature inside the stator and spectra were taken on increasing the temperature every 5°C. Figure 7 gives the spectra at room temperature of the unmelted polycrystalline compound and of the cycled sample. It is clear that two crystalline solids in nearly equal amount are obtained after melting. Many peaks within the spectrum are doubled. For example, four peaks are obtained in the −OCH$_2$− region. Two peaks have the same chemical shift as that for the unmelted compound. In addition, in the most shielded part of the aromatic region Ca and Cb present four peaks. On heating, the

two −OCH$_2$− peaks corresponding to the Cr2 molecules are disappearing near 75°C and are replaced by the signals of the nematic phase.

4.   Conclusion

The structures of two compounds containing four rings in the main core and two lateral chains are presented. In both structures the four ring central core is extended and quite rigid, with a total length close to 28.5 Å. In both structures the alkoxy lateral chains are folded back along the core; they exhibit slightly different conformations and are quite disordered. The molecular arrangement is characteristic of a nematogenic system.

The ^{13}C MAS NMR spectra of four compounds having the same central core were obtained upon temperature increase. In the solid phase the −OCH$_2$− frequencies are different, showing that this signal cannot be used to probe the chain conformation in the solid phase. At the solid–nematic transition, the frequencies of the first two lateral carbons in the four compounds are nearly the same, indicating that the mean chain conformation in the nematic phase is rather independent of the chain length and the far part of the molecule. On cooling, different types of solids can be obtained corresponding to different conformations for the chains. This is supported by other X-ray structures of dilaterally substituted compounds with longer chains, showing that it is possible to obtain different chain conformations in the crystalline phase from those published in this paper for short chains.

References

[1] WEISSFLOG, W., and DEMUS, D., 1983, *Cryst. Res. Tech.*, **18**, K21.
[2] WEISSFLOG, W., and DEMUS, D., 1984, *Cryst. Res. Tech.*, **19**, 55.

[3] WEISSFLOG, W., and DEMUS, D., 1985, *Mol. Cryst. liq. Cryst*., **129,** 235.

[4] DEMUS, D., 1989, *Liq. Cryst*., **5,** 75.

[5] ATTARD, G. S., and IMRIE, C. T., 1989, *Liq. Cryst*., **6,** 387.

[6] NGUYEN, H. T., and DESTRADE, C., 1989, *Mol. Cryst. liq. Cryst. Lett.*, **6,** 123.

[7] BERDAGUÈ, P., PEREZ, F., JUDEINSTEIN, P., and BAYLE, J.-P., 1995, *New. J. Chem*., **19,** 293.

[8] BERDAGUÈ, P., PEREZ, F., BAYLE, J.-P., HO, M. S., and FUNG, B. M., 1995, *New. J. Chem*., **19,** 383.

[9] PEREZ, F., JUDEINSTEIN, P., BAYLE, J.-P., ROUSSEL, F., and FUNG, B. M., 1997, *Liq. Cryst*., **22,** 711.

[10] PEREZ, F., JUDEINSTEIN, P., BAYLE, J.-P., ROUSSEL, F., and FUNG, B. M., 1998, *Liq. Cryst*., **24,** 627.

[11] PEREZ, F., JUDEINSTEIN, P., and BAYLE, J.-P., 1995, *New. J. Chem*., **19,** 1015.

[12] PEREZ, F., BAYLE, J. P., and FUNG, B. M., 1996, *New. J. Chem*., **20,** 537.

[13] NORTH, A. C. T., PHILIPS, D. C., and MATHEWS, F. S., 1968, *Acta. Cryst*., **A24,** 351.

[14] GILMORE, C. J., 1984, *Appl. Cryst*., **17,** 42.

[15] SHELDRICK, G. M., 1993, Program for the Refinement of Crystal and Molecular, University of Göttingen, Germany.

[16] HAW, J. F., 1988, *Anal. Chem*., **559A,** 60.

[17] BERDAGUÈ, P., MUNIER, M., JUDEINSTEIN, P., BAYLE, J.-P., NAGARAJA, C. S., and RAMANATHAN, K. V., 1999, *Liq. Cryst*., **26,** 211.

[18] DAVIES, K., 1983, Snoopi, Program for Drawing Crystal and Molecular Diagrams, Chemistry Laboratory, University of Oxford, England.

[19] ALLOUCHI, H., COTRAIT, M., GUILLON, D., HEINRICH, B., and NGUYEN, H. T., 1995, *Chem. Mater.,* **7,** 2252.

[20] ALLOUCHI, H., BIDEAU, J. P., COTRAIT, M., DESTRADE, C., and NGUYEN, H. T., 1994, *Mol. Cryst. liq. Cryst*., **239,** 153.

[21] PEREZ, F., BERDAGUÈ, P., JUDEINSTEIN, P., BAYLE, J.-P., ALLOUCHI, H., CHASSEAU, D., COTRAIT, M., and LAFONTAINE, E., 1995, *Liq. Cryst*., **19,** 345.

[22] PEREZ, F., BERDAGUÈ, P., JUDEINSTEIN, P., BAYLE, J.-P., ALLOUCHI, H., COTRAIT, M., and LAFONTAINE, E., 1996, *Liq. Cryst*., **21,** 855.

[23] PEREZ, F., JUDEINSTEIN, P., BAYLE, J.-P., ALLOUCHI, H., COTRAIT, M., ROUSSEL, F., and FUNG, B. M., 1998, *Liq. Cryst*., **24,** 627.

[24] CANLET, C., FUNG, B. M., ROUSSEL, F., LEBLANC, K., BERDAGUÈ, P., and BAYLE, J.-P., *Liq. Cryst*. (in the press).